

Vortex states in rotating $^3\text{He-A}$ in a weak magnetic field

Xenophon Zotos and Kazumi Maki

Department of Physics, University of Southern California, Los Angeles, California 90089-0484

(Received 5 October 1984)

We study theoretically the phase diagram of vortex states in $^3\text{He-A}$ in a weak magnetic field $H \sim H_0$ (30 Oe). We find that the lattice of 2π analytic vortices proposed by Fujita *et al.* has the lowest free energy for $H \ll H_0$, while for $H \gg H_0$ the lattice of vortex pairs (Seppälä-Volovik vortices) is more favorable. In the vicinity of the transition temperature ($T > 0.8T_c$) the lattice of dipole-locked vortex pairs appears between the above two configurations in a magnetic field $H \sim 0.5H_0$ and for a rotation speed $\Omega \lesssim 0.04$ rad/sec.

I. INTRODUCTION

The recent NMR experiment on rotating $^3\text{He-A}$ by Hakonen *et al.* has greatly advanced our understanding on the vortex structure.¹ It is now established both experimentally and theoretically that in a high magnetic field ($H \simeq 10H_0$, where $H_0 \sim 30$ Oe is the magnetic field equivalent to the dipole-orientation field) the lattice of Seppälä-Volovik (SV) vortices has the lowest free energy.²⁻⁵ On the other hand in a low magnetic field ($H < H_0$) the square lattice formed by 2π vortices⁶ has the lowest free energy.

The purpose of this paper is to construct the phase diagram for different vortex structures as a function of vortex density n_v (or the rotation speed), reduced magnetic field H/H_0 , and reduced temperature T/T_c . In the course of the present analysis we have discovered a third possibility; the lattice of dipole-locked vortex pairs (DLP) which has the lowest free energy in a narrow window in magnetic field for $T > 0.75T_c$ and for $r_0/\xi_\perp > 70$, where $r_0(\pi n_v)^{-1/2}$ is the intervortex distance and $\xi_\perp \simeq 10 \mu\text{m}$ is the dipole coherence length. At lower temperatures the lattice of SV vortices appears to transform directly into

the square lattice of 2π vortices as the magnetic field is decreased. The ultrasonic attenuation experiment can provide the most direct probe to observe the predicted textural transformation, since the asymptotic direction of \hat{l} away from the vortex centers is unidirectional for the SV vortex lattice, while it becomes bidirectional (i.e., it spreads uniformly in the plane perpendicular to the rotation axis) for the 2π vortex lattice. Therefore, the attenuation coefficient should experience a sudden jump at the transition from one vortex structure to the other.

II. FREE-ENERGY ANALYSIS

We shall evaluate separately the free energies for the three vortex structures within the Wigner-cell approximation. We limit ourselves to the lattices formed by the circular and the hyperbolic vortices as these lattices have lower energy than the corresponding ones with the radial and the hyperbolic vortices. We shall start with the generalized Ginzburg-Landau free energy as given by Cross,⁷ where the coefficients are evaluated within the weak-coupling theory⁸ with the Fermi-liquid coefficients as determined by Greywall.⁹

$$f = \frac{1}{2} \chi_N C_1^2 \int d^3r \{ k_1 (\hat{l} \cdot \nabla \Phi)^2 + k_2 (\hat{l} \times \nabla \Phi)^2 + k_3 (\nabla \Phi) [\text{curl} \hat{l} - \hat{l} (\hat{l} \cdot \text{curl} \hat{l})] - k_4 (\nabla \Phi) \cdot \hat{l} (\hat{l} \cdot \text{curl} \hat{l}) + k_5 (\text{div} \hat{l})^2 + k_6 (\hat{l} \times \text{curl} \hat{l})^2 + k_7 (\hat{l} \cdot \text{curl} \hat{l})^2 + |(\hat{l} \times \nabla) \hat{d}|^2 + \lambda |(\hat{l} \cdot \nabla) \hat{d}|^2 + \xi_\perp^{-2} [1 - (\hat{l} \cdot \hat{d})^2] + \xi_H^{-2} \hat{d}_z^2 \} , \quad (1)$$

where

$$\nabla \Phi = \nabla \alpha + \cos \beta \nabla \gamma . \quad (2)$$

α is the phase of the order parameter and the orbital vector \hat{l} is defined in terms of the Euler angles β, γ as follows:

$$\hat{l} = (-\sin \beta \cos \gamma) \hat{x} + (\sin \beta \sin \gamma) \hat{y} + \cos \beta \hat{z} , \quad (3)$$

while the magnetic \hat{d} vector is defined as

$$\hat{d} = (-\sin \chi \cos \psi) \hat{x} + (\sin \chi \cos \psi) \hat{y} + \cos \chi \hat{z} . \quad (4)$$

The last two terms in Eq. (1) are the dipole energy and the magnetic energy, with $\xi_H = (H_0/H) \xi_\perp$ and we take the magnetic field in the \hat{z} direction parallel to the rotation axis.

A. Seppälä-Volovik vortex

We have already analyzed extensively the free energy of this texture in Refs. 3 and 4. Therefore, we shall summa-

size the relevant results here. We use a hyperbolic coordinate system (u, v) defined by

$$\begin{aligned} x &= c \cosh u \cos v, \\ y &= c \sinh u \sin v. \end{aligned} \quad (5)$$

$2c$ is the distance between vortices in a pair. We parametrize the angles $\alpha, \beta, \gamma, \psi$, and χ as follows:³

$$\begin{aligned} \alpha &= \phi_1 + \phi_2, \quad \gamma = -\phi_1 + \phi_2 + \pi/2, \\ \phi_1 &= \tan^{-1} \left[\frac{y}{x-c} \right], \quad \phi_2 = \tan^{-1} \left[\frac{y}{x+c} \right], \\ \cos \beta &= \cos v e^{-a(\cosh u - 1)}, \\ \chi &= \pi/2, \quad \psi \simeq \pi/2. \end{aligned} \quad (6)$$

c and a are variational parameters, a dictates the approach of \hat{l} to the \hat{x} - \hat{y} plane from the vertical direction at the center of the vortices. The magnetic vector \hat{d} lies in the \hat{x} - \hat{y} plane practically parallel to the \hat{y} direction, asymptotic direction of the \hat{l} vector. The free energy per unit length for a pair is given by

$$\begin{aligned} f_1 &= (f/\pi\chi_N C_1^2) = 4(k_1 + k_2) \ln(r_0/\xi_1) + \Delta f_1 \\ &= A_1 \ln(r_0/\xi_1) + \Delta f_1. \end{aligned} \quad (7)$$

r_0 is the intervortex distance related to the density of 4π vortices n_v and the rotation speed Ω by

$$r_0 = (\pi n_v)^{-1/2} = (h/2\pi m_3 \Omega)^{1/2}.$$

In Fig. 1 we present the results for the temperature dependence of Δf_1 , a , and \bar{c}/ξ_1 . The coefficient $A_1 = 4(k_1 + k_2)$ of the logarithmic term is readily interpreted as due to the circulation considering the asymptotic unidirectionality of the \hat{l} vector and the 4π vorticity of the vortex pair.

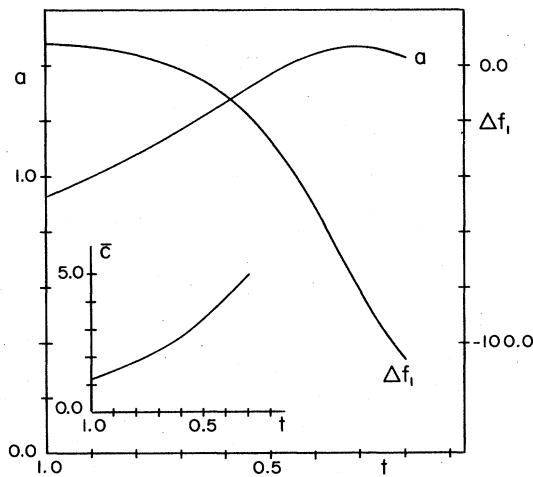


FIG. 1. Free energy Δf_1 , a , and $\bar{c} = c/\xi_1$ as a function of temperature $t = T/T_c$ for the SV vortex pair.

B. Dipole-locked vortex pair

In a high magnetic field the stability of the Seppälä-Volovik vortex pair, where \hat{d} lies in the \hat{x} - \hat{y} plane, is guaranteed by the gain in magnetic energy despite the loss in dipole energy near the center of the vortices. Therefore by decreasing the magnetic field at $H \sim H_0$ we expect a textural transition where the \hat{d} vector becomes practically parallel to the \hat{l} vector. In the following we will examine only the dipole-locked case as we expect it to be a very good approximation in a weak magnetic field. We use the same variational functions as for the SV vortex except that we take $\chi = \beta$ and $\psi = \gamma$ (i.e., $\hat{l} \parallel \hat{d}$). The free energy is given by

$$\begin{aligned} f_2 &= 4(k_1 + k_2) \ln(r_0/\xi_H) + \Delta f_2 \\ &= A_1 \ln(r_0/\xi_H) + \Delta f_2. \end{aligned} \quad (8)$$

Now the length scale is the magnetic coherence length ξ_H so that the logarithmic term and the vortex distance c are scaled by ξ_H . The temperature dependence of Δf_2 , c/ξ_H , and a is shown in Fig. 2. As expected when the vortex pair becomes dipole locked, $2c$ increases to an intervortex distance roughly 4 times larger than that in the SV pair.

C. 2π single analytic vortices (S)

We shall calculate the free energy of the single circular and hyperbolic vortices separately and then we will sum them to compare with the vortex pairs. We use cylindrical coordinates (r, ϕ) and we parametrize the Euler angles (α, β, γ) as follows:¹⁰

$$\begin{aligned} \alpha &= \phi, \\ \cos \beta &= \cos \gamma = e^{-a_c r}, \quad \gamma = \psi = -\phi + \frac{\pi}{2} \text{ for circular,} \\ \cos \beta &= \cos \gamma = e^{-a_h r}, \quad \gamma = \psi = \phi \text{ for hyperbolic.} \end{aligned} \quad (9)$$

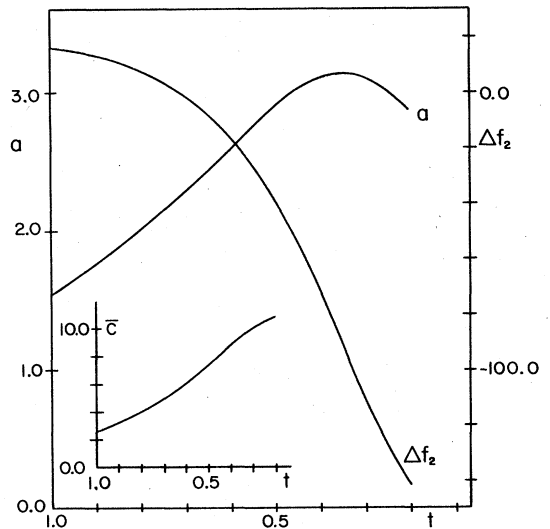


FIG. 2. Free energy Δf_2 , a , and $\bar{c} = c/\xi_H$ as a function of temperature $t = T/T_c$ for the dipole-locked vortex pair.

We again consider only the dipole-locked case and we take r'_0 corresponding to rotation speed Ω related to r_0 by $r'_0 = r_0/\sqrt{2}$. The free energies of the two vortices are given by

$$\begin{aligned} f_c &= 4(k_1 + k_6 + \lambda)\ln(r'_0/\xi_H) + \Delta f_c, \\ f_h &= 2(k_1 + k_2 + k_5 + k_6 + 1 + \lambda)\ln(r'_0/\xi_H) + \Delta f_h, \quad (10) \\ f_3 &= f_c + f_h = A_2\ln(r'_0/\xi_H) + \Delta f_3. \quad (11) \end{aligned}$$

The results for Δf_3 , $a_c\xi_H$, and $a_h\xi_H$ are plotted in Fig. 3.

III. PHASE DIAGRAM

We can qualitatively understand the vortex phase diagram by considering first the logarithmic terms in the free energy. The logarithmic term of the SV vortex pair scales with ξ_\perp while those of the 2π single or DLP scale with ξ_H . Therefore we expect that at high magnetic fields the SV vortex is more favorable and that there is a textural phase transition to dipole-locked single or DLP vortices at lower field of the order of H_0 . To determine the phase boundary between the lattice of the SV vortices and that of 2π vortices we equate the free-energy expressions (7) and (11) and we obtain

$$r_0/\xi_\perp = \delta(H/H_0)^\epsilon, \quad (12)$$

where

$$\delta = \exp\left[\frac{\Delta f_3 - \Delta f_1}{A_1 - A_2}\right]$$

and the exponent $\epsilon = A_2/A_1 - A_2$. The temperature dependence of the coefficients A_1 and A_2 is shown in Fig. 4. Near T_c $A_1 < A_2$ so that ϵ is negative, near $T \approx 0.75T_c$ $A_1 = A_2$ so the exponent ϵ diverges. At this temperature the critical field which separates the SV vortex from the 2π vortex lattice becomes independent of the vortex density n_v . For $T < 0.75T_c$ the exponent becomes

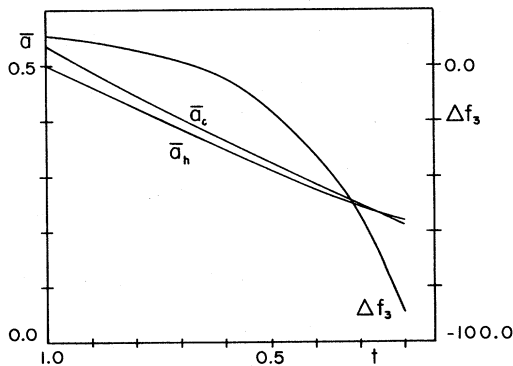


FIG. 3. Free energy Δf_3 , $\bar{a}_c = a_c\xi_H$, and $\bar{a}_h = a_h\xi_H$ as a function of temperature $t = T/T_c$ for circular and hyperbolic single (S) 2π vortices.

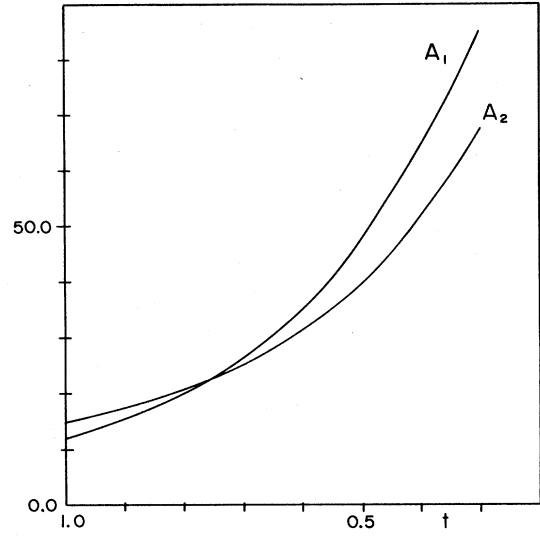


FIG. 4. Free-energy logarithmic term coefficients A_1 and A_2 as a function of temperature $t = T/T_c$.

positive. In Table I we give the values of δ and ϵ for several temperatures.

In passing we should note that the coefficient δ depends on the energies Δf_1 and Δf_3 which reflect the internal structure of the vortices. As we are using a variational method we can only attach a semiquantitative meaning to these coefficients. On the other hand, the exponent ϵ depends on the k_i coefficients of Cross's free-energy expression; they are calculated within the weak-coupling theory which is believed accurate within 10%. Then, it would not be difficult to determine experimentally the field dependence of the phase boundary lines.

Comparing the coefficients of $\ln(r_0/\xi_H)$ for the 2π vortices and DLP we can conclude immediately that in the dilute limit the latter is more stable for T close to T_c while at lower temperatures the 2π vortex lattice is always favored. At first sight the DLP appears to become more stable than the 2π vortices in the high-density limit for $T \leq 0.73T_c$. However, it is easy to see that in this region, where $r_0 \leq 20\xi_\perp$, our calculation is no longer valid as interaction between vortices should be taken into account. Therefore for $T \leq 0.75T_c$ the DLP cannot be stable for any vortex density.

TABLE I. Values of δ and ϵ for several temperatures.

T/T_c	δ	ϵ
1.0	2.4	-5.0
0.8	164.0	-21.0
0.6	0.3	+7.8
0.4	1.1	+3.8
0.2	0.44	+5.4

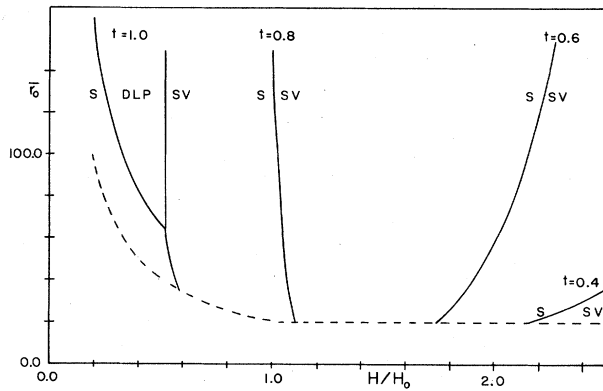


FIG. 5. Vortex phase diagram as a function of $\bar{r}_0=r_0/\xi_{\perp}$ and magnetic field H/H_0 , at several temperatures $T=T/T_c$. The dotted line denotes the limit of validity of the calculation.

IV. CONCLUSION

We have compared the free energies of three possible vortex configurations, the lattice of SV vortices, that of DLP and that of 2π vortices. We find that in a high magnetic field the lattice of SV vortices has the lowest free energy, while in a small magnetic field that of 2π vortices has the lowest free energy. Furthermore, for $T \geq 0.75T_c$

and for small rotation speed the lattice of DLP becomes stable in a window of magnetic field for $H \sim 0.5H_0$. We have constructed the phase diagram, which can be tested both by NMR and by ultrasonic attenuation experiment (see Fig. 5).

However, although the NMR satellites associated with these three configurations are distinct (note that there will be no satellite associated with DLP as $\hat{\mathbf{l}} \parallel \hat{\mathbf{d}}$ in the equilibrium configuration¹¹), low-field NMR experiments are rather difficult due to the small resonance frequency. Ultrasonic attenuation, on the other hand, will provide clear signature of the transition between the SV vortex lattice and the 2π vortex lattice, since for the SV vortex lattice the asymptotic direction of $\hat{\mathbf{l}}$ away from the vortex center is unidirectional (say, in the $\hat{\mathbf{y}}$ direction) while for the 2π vortex lattice it is bidirectional (spreads in the $\hat{\mathbf{x}}\text{-}\hat{\mathbf{y}}$ plane). The detection of the transition between the SV vortex lattice and the DLP lattice may be somewhat more subtle. However, since the distance between vortices in a pair jumps almost by a factor of 4 associated with this transition, this transition may be as well accessible to the ultrasonic attenuation experiment.

ACKNOWLEDGMENT

This work is supported by the National Science Foundation under Grant No. DMR 82-14525.

¹P. J. Hakonen, O. T. Ikkala, S. T. Islander, O. V. Lounasmaa, and G. E. Volovik, *J. Low Temp. Phys.* **53**, 425 (1983); H. K. Seppälä, P. J. Hakonen, M. Krusius, T. Ohmi, M. M. Salomaa, J. T. Simola, and G. E. Volovik, *Phys. Rev. Lett.* **52**, 1802 (1984).

²H. K. Seppälä and G. E. Volovik, *J. Low Temp. Phys.* **51**, 279 (1983).

³X. Zotos and K. Maki, *Phys. Rev. B* **30**, 145 (1984).

⁴K. Maki and X. Zotos, *Phys. Rev. B* **31**, 177 (1985).

⁵See, however, Ref. 2 and A. L. Fetter, J. A. Sauls, and D. L.

Stein, *Phys. Rev. B* **28**, 5061 (1983), where it is asserted that the 2π singular vortices are more stable based on approximate numerical analysis.

⁶T. Fujita, M. Nakahara, T. Ohmi, and T. Tsuneto, *Prog. Theor. Phys.* **60**, 671 (1978); see also, Ref. 5.

⁷M. C. Cross, *J. Low Temp. Phys.* **21**, 525 (1975).

⁸R. Combescot, *J. Low Temp. Phys.* **18**, 537 (1975) and Ref. 5.

⁹D. S. Greywall, *Phys. Rev. B* **27**, 2747 (1983).

¹⁰K. Maki, *Phys. Rev. B* **27**, 4173 (1983).

¹¹R. Bruinsma and K. Maki, *Phys. Rev. B* **18**, 1101 (1978).